Traffic 2003; **4**: 857–868
Blackwell Munksgaard

doi: 10.1046/j.1600-0854.2003.00140.x

The Ubiquitin-Vacuolar Protein Sorting System is Selectively Required During Entry of Influenza Virus into Host Cells

Rebecca Khor, Lisa J. McElroy and Gary R. Whittaker*

Department of Microbiology & Immunology, Cornell University, Ithaca NY 14853, USA
** Corresponding author: Gary R. Whittaker, grw7@cornell.edu*

Influenza virus enters cells by endocytosis, and requires the low pH of the late endosome for successful infection. Here, we investigated the requirements for sorting into the multivesicular body pathway of endocytosis. We show that treatment of host cells with the proteasome inhibitors MG132 and lactacystin directly affects the early stages of virus replication. Unlike other viruses, such as retroviruses, influenza virus budding was not affected. The requirement for proteasome function was not shared by two other pH-dependent viruses: Semliki Forest virus and vesicular stomatitis virus. With MG132 treatment, incoming influenza viruses were retained in endosomes that partially colocalized with mannose 6-phosphate receptor, but not with classical markers of early or late endosomes. Colocalization was also observed with Rme-1, which is part of the recycling pathway of endocytosis. In addition, influenza virus entry was dependent on the vacuolar protein sorting pathway, as over-expression of dominant-negative hVPS4 caused arrest of viruses in endosome-like populations that partially colocalized with the hVPS4 protein. Overall, we conclude that influenza virus selectively requires the ubiquitin/vacuolar protein sorting pathway for entry into host cells, and that it must communicate with a specific cellular machinery for intracellular sorting during the initial phase of virus infection.

Key words: endocytosis, endosomal sorting, influenza virus, ubiquitin, Vps4

Received 18 August 2003, revised and accepted for publication 16 September 2003

Within the cell, protein ubiquitylation is classically associated with targeting of proteins for degradation by the 26S proteasome (1). Such modification requires the addition of multiple ubiquitin moieties (4 or more) to proteins, or polyubiquitylation. More recently, however, other functions of ubiquitin have emerged – which include a role in membrane traffic, especially internalization from the plasma membrane and endocytic sorting [reviewed in (2)]. In contrast to proteasome-directed polyubiquitylation, the function of the ubiquitin tag in the endocytic pathway requires only a single ubiquitin event, termed monoubiquitylation. In yeast, monoubiquitylation is well established to regulate internalization of receptors such as the G-protein coupled receptors alpha factor and Ste2 (3), and to control the function of the vacuole (the yeast equivalent of the mammalian lysosome) [reviewed in (4,5)]. In mammalian cells, ubiquitylation is generally thought to be dispensable for internalization itself, but is required for sorting into late endosomes and the lysosome-targeted pathway of endocytosis [reviewed in (6,7)]. Such sorting occurs via the 'inwards' budding of membrane into so-called multivesicular bodies (MVBs) (8).

In mammalian cells, a role for ubiquitylation in endocytosis is exemplified by the epidermal growth factor receptor (EGFR), which upon monoubiquitylation of its cytoplasmic tail is sequestered into the internal vesicles of the MVB, ready for degradation in the lysosome (8). Defects in ubiquitylation result in decreased EGFR degradation, missorting to the recycling pathway of endocytosis, and a loss of signal attenuation (9). Other receptors that show a similar involvement of the ubiquitin system for intracellular sorting and/or degradation include the β_2 adrenergic receptor, the growth hormone receptor (GHR) and the interleukin 2 receptor (IL2R) β chain (10–13).

Because of its role in 'inwards' budding in MVBs, ubiquitylation has also been studied in regard to virus budding at the plasma membrane (also an 'inwards' budding event relative to budding of intracellular membranes) [reviewed in (2,14)]. Many enveloped viruses, encompassing retroviruses (e.g. human immunodeficiency virus, HIV), rhabdoviruses (e.g. vesicular stomatitis virus, VSV), hantaviruses and filoviruses (e.g. Ebola virus) contain so-called late domains, which are required for budding – and which in many cases are monoubiquitylated during virus assembly (15–22). This ubiquitylation event is essential for virus budding at the plasma membrane, presumably due to a re-localization of the MVB budding machinery to the site of virus assembly and envelopment. In agreement with this, 'late domain'-containing viruses also utilize the vacuolar protein sorting (vps) machinery of the cell during virus budding. Vps components known to play a role for retroviruses and Ebola virus include TSG101 (the homolog of Vps23p in yeast), VPS28 and VPS4 (18,19,22–24).

Many viruses utilize endocytosis for entry into host cells (25,26). In addition to a role in budding, viruses may therefore utilize ubiquitin and the vacuolar protein sorting

pathway during their entry. We have previously shown that unlike most pH-dependent enveloped viruses that enter cells by endocytosis, influenza virus (an orthomyxovirus) requires entry into the late endosome for productive infection (27). Here, we address the role of ubiquitylation and endosomal sorting during influenza virus replication. Using a combination of pharmacological, molecular and morphological approaches, we show that both protein ubiquitylation and the vps pathway are specifically required for entry and productive infection of influenza virus. Other pH-dependent endocytic viruses (Semliki Forest virus, or SFV, as well as VSV) that do not require functional late endosomes for entry (27,28), do not require the ubiquitin-vps system for infection. Despite a requirement for budding from the plasma membrane late in infection, ubiquitylation is not required for influenza virus assembly or release.

Results

Treatment with MG132 inhibits influenza virus replication at an early stage of infection

As an initial way to examine the effects of ubiquitylation on influenza virus replication, we treated cells with the proteasome inhibitor MG132, a peptide aldehyde which is well established as a cell biological tool that is a potent transition state inhibitor of proteasome activity (29). MG132 has recently been applied to study the role of ubiquitylation in endosomal transport and virus budding (8,30–34). We treated cells with MG132, or left them untreated, and then infected them with influenza virus. Virus infection was monitored by expression of influenza virus nucleoprotein (NP), using immunofluorescence microscopy. In the absence of drug, we observed strong expression of NP in the nucleus (Figure 1A, panel a). Treatment of infected cells with MG132 led to a dramatic reduction in viral protein expression in the nucleus, with the virus apparently arrested in a punctate cytoplasmic location (Figure 1A, panel b). To confirm that our observed effects on virus infection were due to defective proteasome activity, we utilized an alternative inhibitor, lactacystin – which acts as a covalent modifier of the proteasome (29). Immunofluorescence microscopy of influenza-infected cells treated with lactacystin also showed a pronounced effect of the inhibitor on virus replication (Figure 1A, panel c).

To quantitate our microscopy results with MG132, virus infection was monitored by expression of a late viral

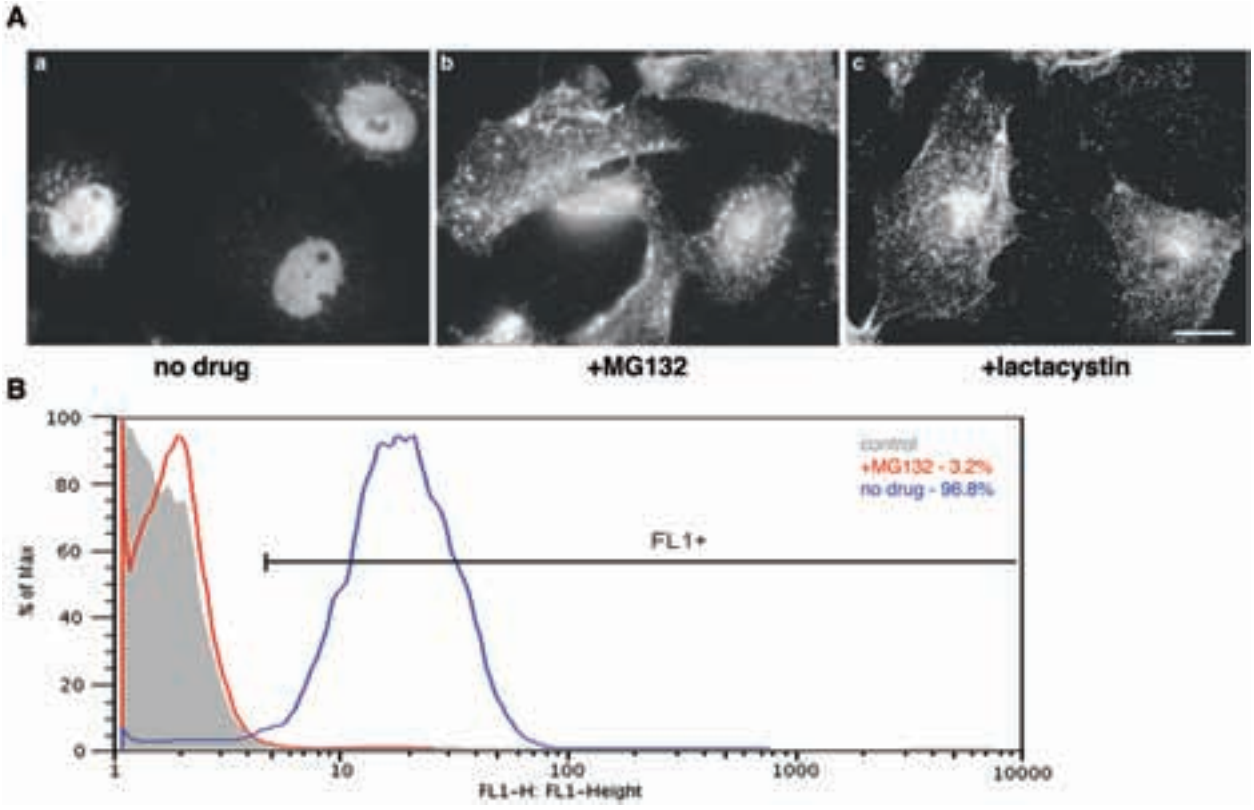

Figure 1: (A) Mv 1 Lu cells were treated in the absence of drug (a), with 10 μM MG132 (b), or with 40 μM lactacystin (c), and infected with approximately 1–5 pfu/cell influenza virus (WSN). Cells were fixed at 2.5 h post infection and analyzed by immunofluorescence microscopy. Bar = 10 μm. (B) Mv 1 Lu cells were treated with 10 μM MG132, or remained untreated (no drug), and infected with approximately 1–5 pfu/cell influenza virus (WSN). Cells were fixed at 5 h post infection and analyzed by flow cytometry. Control cells represent uninfected cells. FL1 + represents the gate used to score positive cells.

glycoprotein (neuraminidase, NA) using flow cytometry. Treatment of infected cells with MG132 led to a dramatic reduction in viral protein expression. In untreated cells, 97% of cells showed NA expression, whereas in cells treated with MG132, less than 2% of the cells expressed NA (Figure 1B).

To examine in more detail the point in the replication cycle that proteasome inhibitors might have their effect, we infected cells and then treated them with MG132 after 2 h of infection (a time point where virus has entered the cell, but shows little or no genome replication). When treated at 2 h after infection, a significant population of cells now expressed high levels of NA – levels similar to those on mock-treated cells (not shown), as shown using immunofluorescence microscopy with anti-NA antibodies (Figure 2). A fraction of cells were still inhibited for NA expression, most likely due to nonspecific effects of the inhibitor when cells were treated for long periods; however, those cells showing normal levels of NA expression show no obvious nonspecific effects on virus replication under our experimental conditions. Overall, these results show that inhibition of proteasome activity, e.g. by using MG132, affects an early event in influenza virus replication, presumably during virus entry.

MG132 does not affect influenza virus budding or release

Many enveloped viruses that bud from the plasma membrane, including retroviruses, rhabdoviruses and filoviruses, appear to rely on ubiquitylation for the budding process (17,21,24,35). In principle, influenza virus (also an enveloped virus that is released from the plasma membrane) might be expected to show ubiquitin-dependent budding. To address this issue, we treated influenza-infected cells with MG132 at 5 h post infection, and monitored released virus particles after 18 h of infection using a hemagglutination assay (Figure 3). As Mv 1 Lu cells showed relatively low levels of released particles, we repeated the experiment using MDBK cells, which gave higher levels of released virions. The addition of MG132 had no effect on the amount of virus particles released from either cell type in three independent experiments. Thin-section electron microscopy of Mv 1 Lu cells showed the presence of budding viruses in both treated and non-treated cells (not shown). These data confirm an earlier report that showed no effect on MG132 or lactacystin on influenza budding (36), and indicate that protein ubiquitylation is not involved in influenza virus budding or release.

Treatment with MG132 does not affect early events in Semliki Forest virus or vesicular stomatitis virus replication

We next wished to address the question of whether the MG132-induced block in the early events of influenza virus replication was shared by other viruses that enter cells in a similar manner. We therefore examined the replication of Semliki Forest virus (SFV) and vesicular stomatitis virus (VSV) replication. Like influenza virus, both SFV and VSV are known to enter cells by pH-dependent endocytosis (37). Treatment of cells with MG132 prior to infection had no significant effect on the expression of viral glycoproteins for either SFV or VSV (Figure 4), showing that ubiquitylation is not universally required for viral endocytosis, but appears selective for influenza virus.

MG132 prevents influenza virus entry into the nucleus and sequesters the virus in endocytic compartments

As our observed effects of MG132 were most likely occurring during virus entry, and because of the known effects of MG132 on endocytic sorting, we examined in more

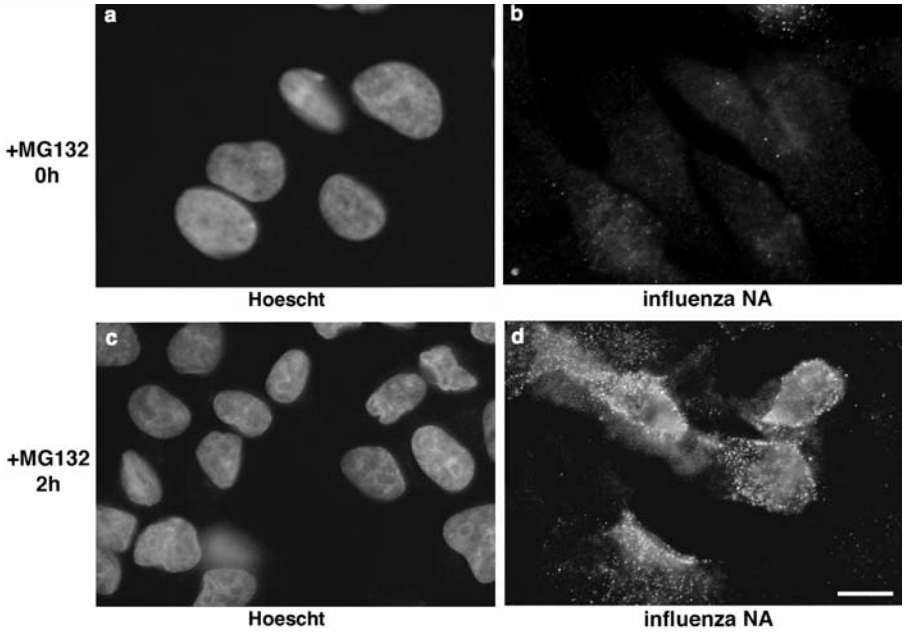

Figure 2: Mv 1 Lu cells were treated with 10 μM MG132 at the time of infection (0 h) (panels a and b), or at 2 h post infection (panels c and d), and infected with approximately 1–5 pfu/cell influenza virus (WSN). Cells were fixed at 5 h post infection and analyzed by immunofluorescence microscopy. Bar = 10 μm.

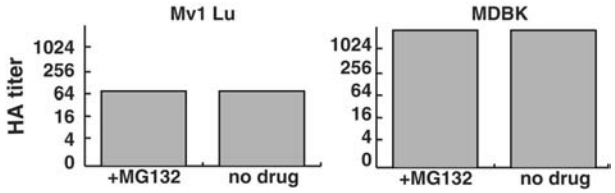

Figure 3: Mv 1 Lu and MDBK cells were infected with approximately 1–5 pfu/cell influenza virus (WSN) and treated with 10 μM MG132 at 5 h post infection, or were untreated (no drug). Cells were harvested at 18 h post infection and supernatant was analyzed by hemagglutination assay. The maximum dilution of virus supernatant that allowed hemagglutination is shown.

detail the effects of the drug on the transit of the influenza virus ribonucleoproteins (vRNPs) through the endocytic network and into the nucleus. We treated cells with MG132 and infected them with influenza virus for approximately 2 h. At this time point, vRNPs would be expected to have transited through both the endosome and cytosol, and entered the nucleus. Cells were fixed, and analyzed by double label confocal microscopy with markers of the endocytic network.

We first analyzed the distribution of vRNPs relative to EEA1, a marker of early endosomes (Figure 5A). In the absence of drug, vRNPs were exclusively localized to the nucleus, and EEA1 was localized to its expected peripheral punctate distribution (Figure 5A, panels a and b). However, when cells were treated with MG132, the vRNPs showed a dramatic redistribution and were now present in a scattered punctate distribution through the cytosol (Figure 5A, panel e). Treatment of cells with MG132 showed no obvious redistribution of EEA1. Alignment of the EEA1 and vRNP signal showed no significant colocalization (Figure 5A, panels f and fí). A very similar pattern was also observed when infected cells were treated with the alternative proteasome inhibitor, lactacystin (not shown).

We next analyzed the distribution of vRNPs relative to the mannose 6-phosphate receptor (M6PR), a marker of late endosomes (Figure 5B). As expected, in the absence of drug, vRNPs were exclusively localized to the nucleus, and M6PR was localized in a perinuclear pattern (Figure 5B, panels a and b). However, when cells were treated with MG132, the vRNPs were again present in a scattered punctate distribution through the cytosol (Figure 5B, panel e). In this case, M6PR also showed a redistribution in the presence of drug and was now also present in a scattered punctate distribution (Figure 5B, panel d). To our knowledge, there are no previous data to show similar redistribution of M6PR in the presence of MG132. Alignment of the M6PR and vRNP signals showed significant, although not complete, colocalization (Figure 5B, panels f and f′). Notably, there were many areas showing signal from vRNPs that did not also contain M6PR, indicating that although much of the virus might be arrested in late endosomes in the presence of MG132, the bulk of the virus was actually in another endosome population.

Rab proteins are known to orchestrate membrane traffic in the cell, and show distinct localizations to specific subcellular compartments (38,39). To investigate further the precise localization of the MG132-arrested virus, we carried out deconvolution wide-field fluorescence microscopy, focusing

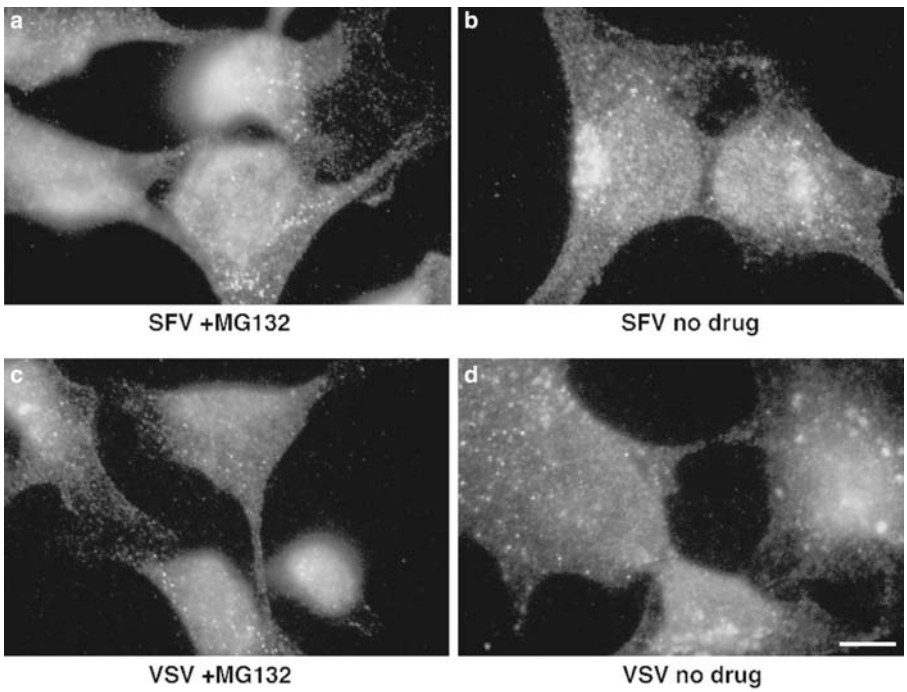

Figure 4: Mv 1 Lu cells were treated with 10 μM MG132, or were untreated (no drug), and infected with approximately 1–5 pfu/cell Semliki Forest virus (SFV) (panels a and b) or vesicular stomatitis virus (VSV) (panels c and d). Cells were fixed at 5 h post infection and analyzed by immunofluorescence microscopy. Bar = 5 μm.

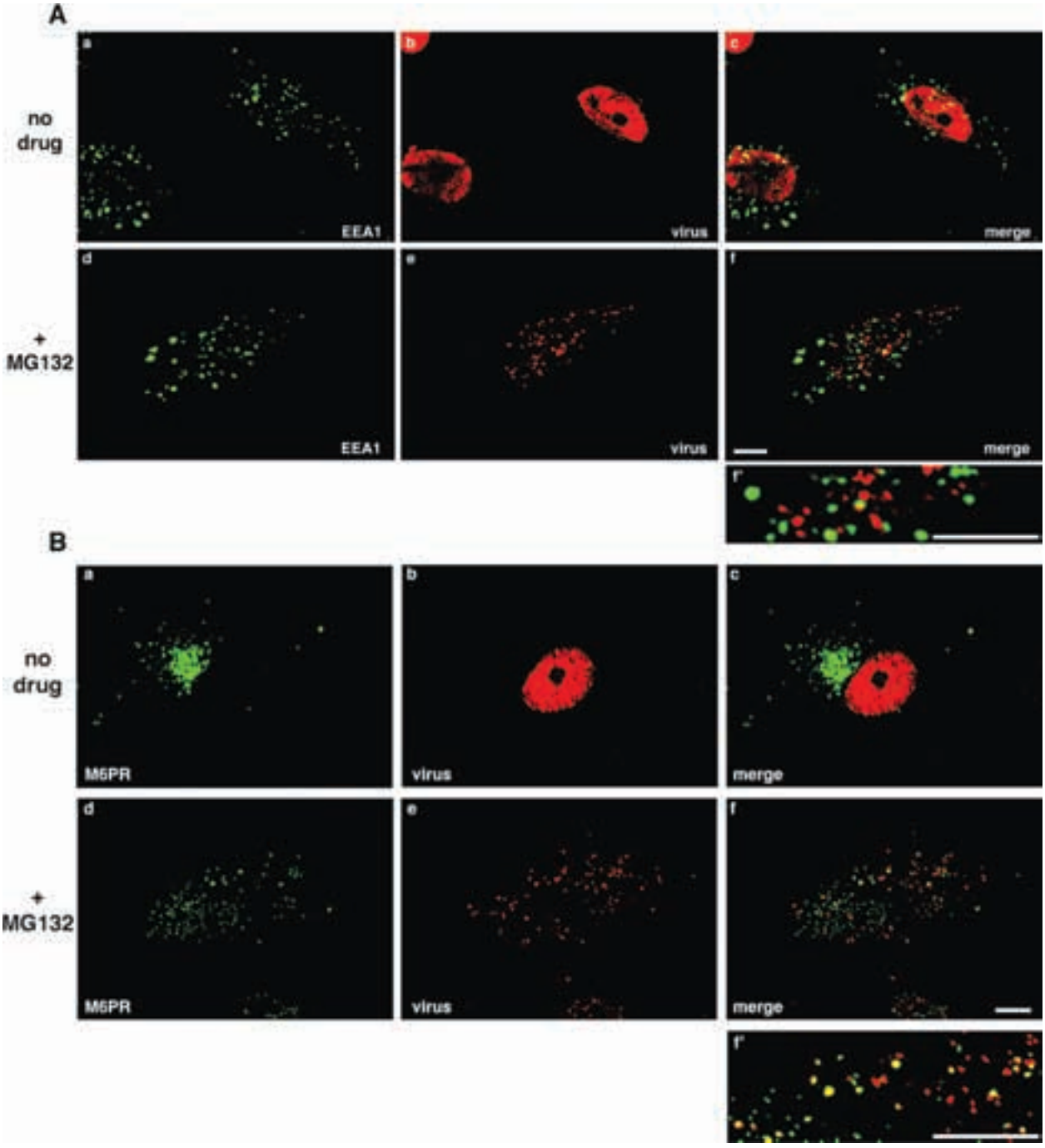

Figure 5: (A) Mv 1 Lu cells were treated with 10 μM MG132 (panels a–c), or were untreated (panels d–f), and infected with approximately 1–5 pfu/cell influenza virus (WSN). Cells were fixed at 2.5 h post infection and analyzed by confocal microscopy using anti-EEA1 antibodies (panels a and d) or anti-influenza virus NP antibodies (panels b and e). Merged images are shown in panels c and f, and an enlargement of a portion of panel f shown in panel (f′) Bars = 10 μm. (B) Mv 1 Lu cells were treated with 10 μM MG132 (panels a–c), or were untreated (panels d–f), and infected with approximately 1–5 pfu/cell influenza virus (WSN). Cells were fixed at 2.5 h post infection and analyzed by confocal microscopy using anti-mannose 6-phosphate (M6PR) antibodies (panels a and d) or anti-influenza virus NP antibodies (panels b and e). Merged images are shown in panels c and f, and an enlargement of a portion of panel f shown in panel f′. Bars = 10 μm.

on Rab proteins known to function in the endocytic pathway. We first examined the localization of virus relative to Rab11 and Rab4, two Rab proteins with characterized functions in recycling endosomes (40). Cells were either labeled for endogenous Rab11 using monoclonal anti-Rab11 antibodies, or transfected with a GFP-tagged Rab4

construct and localization determined by GFP fluorescence. As expected in untreated, infected cells, vRNP signal was almost exclusively nuclear (not shown), whereas in MG132-treated cells vRNPs were scattered in the cytosol; however, neither Rab11 nor Rab4 showed any significant localization with the MG132-arrested vRNPs (Figure 6, panels a and b). Treatment of cells with MG132 showed no obvious redistribution of Rab4 or Rab11.

We next examined the localization of incoming vRNPs relative to Rab9, which has been well established to function in endosome–TGN transport (41). In the absence of drug, vRNPs were exclusively localized to the nucleus and Rab9 was localized in a perinuclear pattern (not shown). When cells were treated with MG132, deconvolution microscopy and alignment of the Rab9 and vRNP signals often showed a distinct pattern of adjacent green and red spots (Figure 6, panel c). Treatment of cells with MG132 showed no obvious redistribution of Rab9. Our data suggested that MG132-arrested vRNPs were present in an endocytic compartment that was connected to, but distinct from, Rab9-positive endosomes.

The adjacent endocytic domains that we observed with MG132-arrested vRNPs and Rab9 resembled the localization previously observed for Rab9 relative to Rab7 (a late endosome Rab protein) (42). We therefore examined the distribution of MG132-arrested vRNPs relative to GFP-Rab7. By double-label deconvolution microscopy, we saw no significant colocalization of influenza vRNPs with Rab7 (Figure 6, panel d), indicating that the virus was not trapped in late endosomes. We further examined MG132-treated cells and examined Rab5, which is present in early endosomes, with no evidence of significant colocalization with incoming vRNPs (Figure 6, panel e). Treatment of cells with MG132 showed no obvious redistribution of Rab7 or Rab5.

To further investigate where the incoming influenza virus particles might be localized in the presence of MG132, we utilized an alternative endocytic marker, Rme-1 – which has previously been shown to be localized to sorting and recycling endosomes (43). Cells were transfected with GFP-Rme-1 and infected with influenza virus in the presence or absence of MG132. In the absence of drug, vRNPs were exclusively localized to the nucleus, and Rme-1 was localized in a scattered cytoplasmic pattern (not shown). When cells were treated with MG132, deconvolution microscopy and alignment of the Rme-1 and vRNP signals showed extensive colocalization (Figure 7).

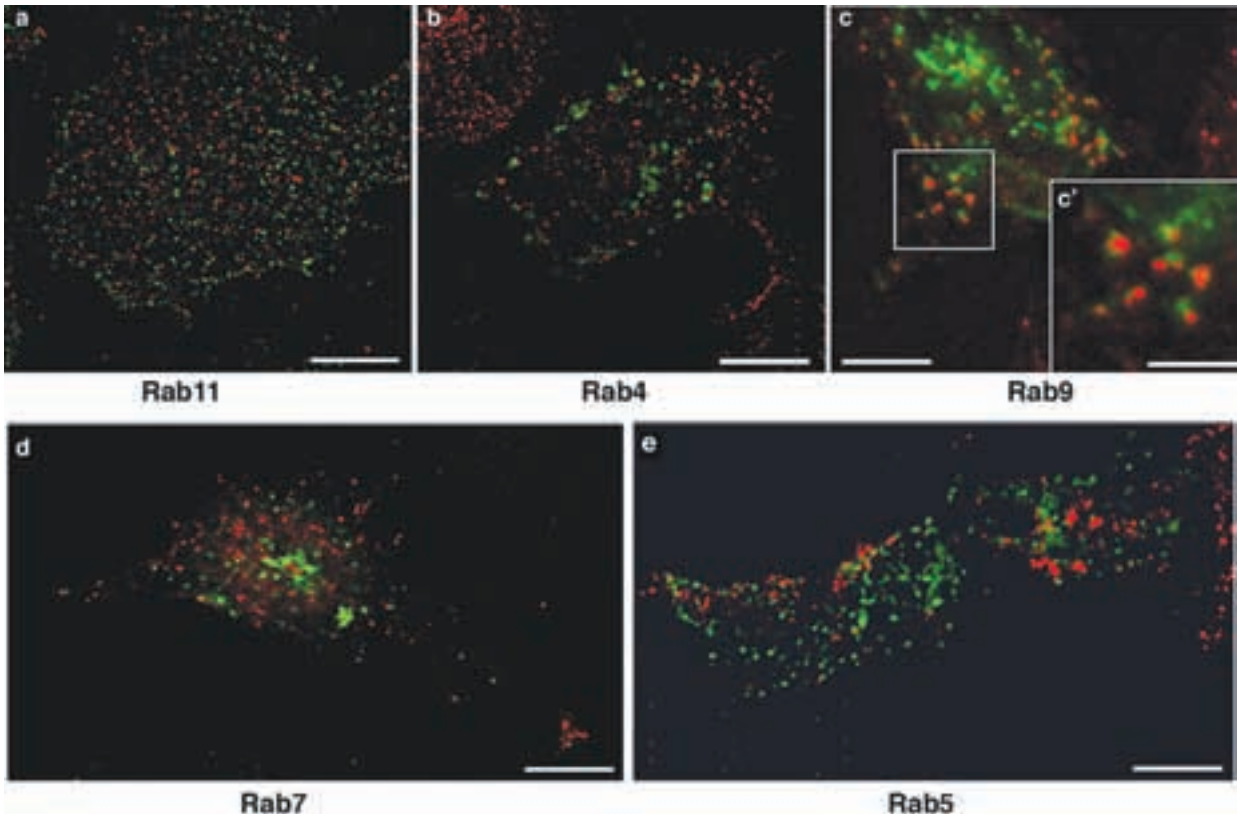

Figure 6: Mv 1 Lu cells were treated with 10 μM MG132, and infected with approximately 1–5 pfu/cell influenza virus (WSN). Cells were fixed at 2.5 h post infection and analyzed by deconvolution microscopy using anti-Rab11 antibodies (panels a) or by intrinsic GFP fluorescence (green), along with anti-influenza virus NP antibodies (red). For panels b–f, cells were transfected with GFP-tagged versions of the indicated Rab proteins 5–6 prior to infection. Merged images are shown. Bars = 10 μm (2 μm in panel f').

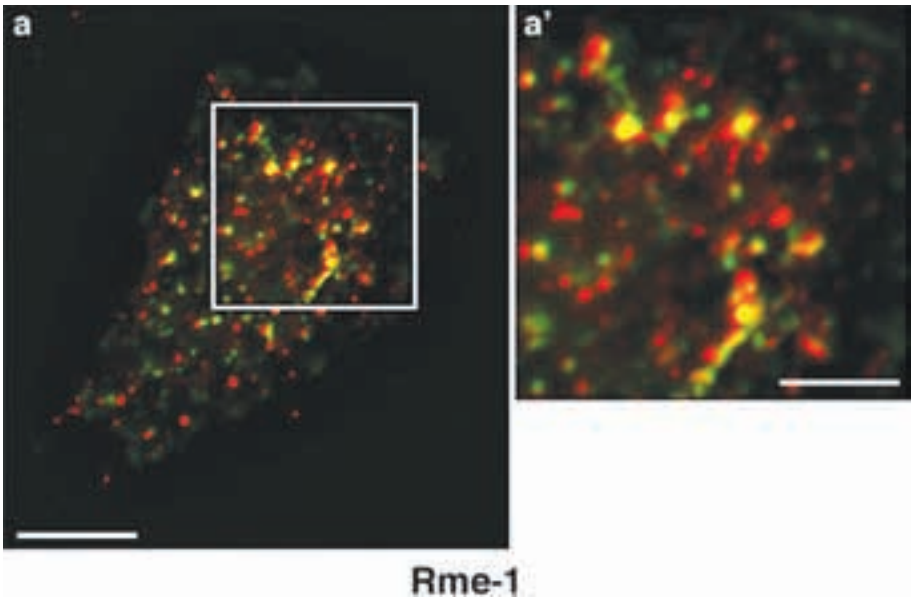

Figure 7: Mv 1 Lu cells were transfected with GFP-tagged Rme-1, treated with 10 μM MG132, and infected with approximately 1–5 pfu/cell influenza virus (WSN). Cells were fixed at 2.5 h post infection and analyzed by deconvolution microscopy using intrinsic GFP fluorescence (green), along with anti-influenza virus NP antibodies (red). Merged images are shown. Bars = 10 μm (2 μm in panel a′).

Colocalization was not complete, as cells did contain regions that did not simultaneously label for both vRNPs and Rme-1.

Overall, these data show that treatment of cells with proteasome inhibitors, such as with MG132, leads to a dramatic arrest in virus entry into the nucleus, and results in the aberrant localization of viruses to endosome populations – which at present we would identify as sorting endosomes.

Dominant-negative human VPS4 prevents influenza virus entry and infection

The yeast and mammalian class E vps proteins are known to recognize ubiquitin and control endocytic sorting (34). Of these, Vps4 has been shown to regulate membrane association of a protein complex required for normal endosome function. Vps4 is an AAA ATPase, and mutation of a conserved glutamic acid (E) to glutamine (Q) results in a mutant protein that is defective in ATP hydrolysis and acts in a dominant-negative manner. Expression of an EQ mutant of the human homolog of the yeast Vps4p (hVPS4 EQ) has been shown to inhibit both retrovirus and Ebola virus budding (19,23,24), as well as endosomal sorting (44).

To examine the role of vps proteins during influenza virus entry, we transfected cells with GFP-tagged versions of wild-type hVPS4, as well as an EQ mutant (E223Q). As reported previously (44), wild-type GFP-hVPS4 was exclusively cytosolic (Figure 8A, panel a), whereas expression of GFP-hVPS4 EQ resulted in the localization of the protein to large vacuoles and bright foci in addition to its cytosolic distribution (Figure 8A, panel c). When we examined influenza virus infection in cells expressing wild-type GFP-hVPS4, the vRNPs were localized exclusively in the nucleus, and were generally indistinguishable from vRNPs in non-transfected cells (Figure 8A, panel b). However, in cells expressing GFP-hVPS4 EQ, vRNPs were not localized to the nucleus, but were present in scattered, large cytosolic puncta (Figure 8A, panel d). This distribution was reminiscent of the MG132-induced localization of influenza virus seen previously. Quantitation of the samples showed that 20.9% of the cells both expressed wild-type hVPS4 and showed a distinct nuclear signal of vRNPs, indicating normal infection, whereas in cells expressing hVPS4 EQ, only 2.5% of the cells were both transfected and infected (Figure 8B).

To examine the localization of vRNPs in cells expressing GFP-hVPS4 EQ in more detail, we performed double-label confocal microscopy (Figure 8C). By this technique, vRNPs were clearly arrested in a scattered cytosolic distribution, which showed significant colocalization with the GFP-hVPS4 EQ protein (Figure 8C, panel c). These data clearly show a functional role of the vacuolar protein sorting pathway in influenza virus entry and infection, and indicate that hVPS4 is required for successful transit of the virus through sorting endosomes.

Discussion

We show here that influenza virus requires the ubiquitin-vacuolar protein sorting system for endocytosis and infection of host cells. This requirement seems to be selective for influenza virus, as it is not required by two other pH-dependent enveloped viruses, Semliki Forest virus (SFV) and vesicular stomatitis virus (VSV). One of the major differences between SFV and VSV, compared to influenza virus, is that their pH for fusion is higher (approximately 6.5, vs. 5.0 for influenza virus). In line with this result, we have recently shown that influenza virus requires both functional early and late endosomes for infection (27). In

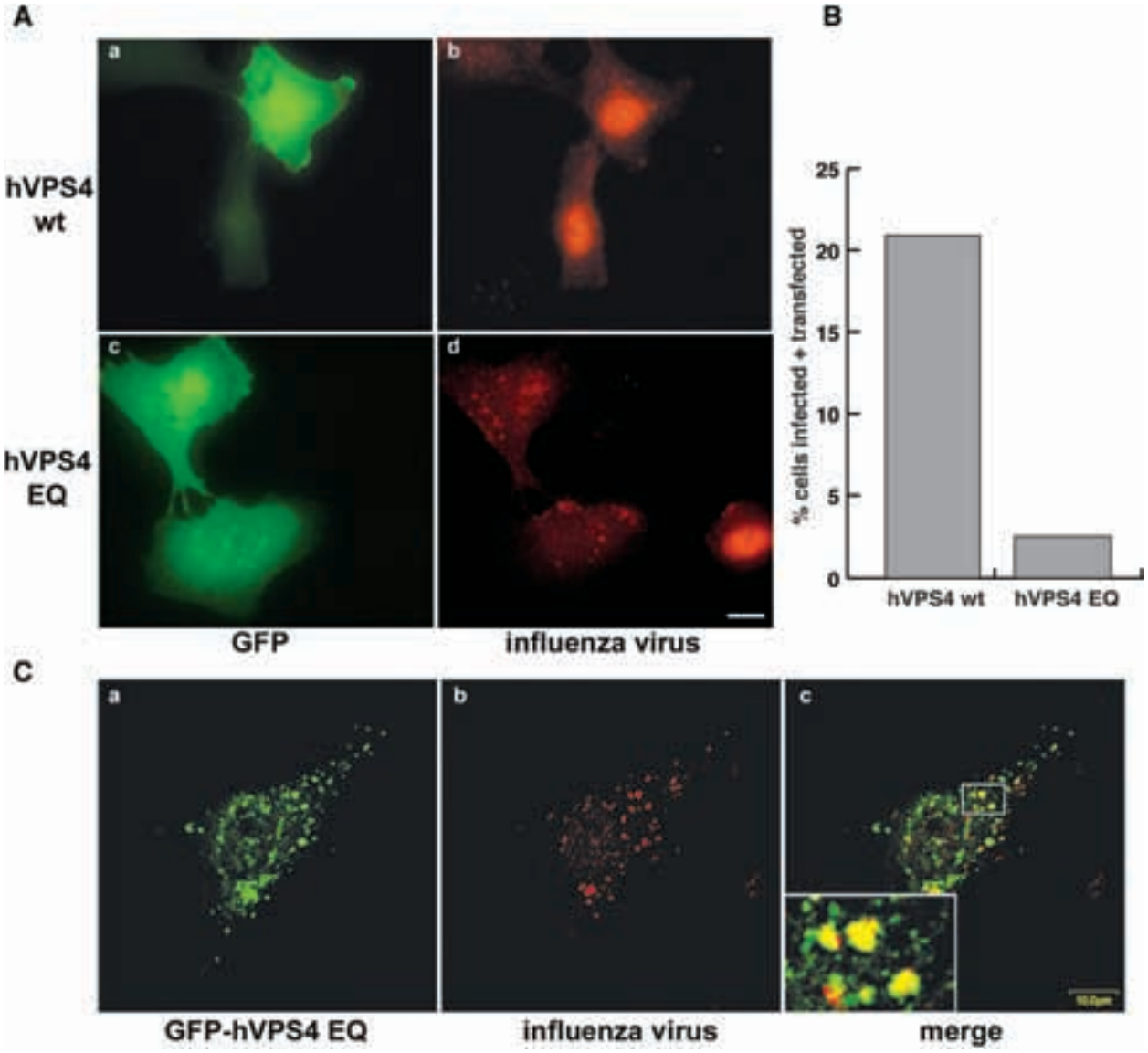

Figure 8: (A) Mv 1 Lu cells were transfected with GFP-tagged hVPS4 wt (panels a and b) or hVPS4 EQ (panels c and d) and then infected with approximately 1–5 pfu/cell influenza virus (WSN). Cells were fixed at 2.5 h post infection and analyzed by immunofluorescence microscopy using intrinsic GFP fluorescence (green), along with anti-influenza virus NP antibodies (red). Bar = 10 μm. (B) Quantitation of results from immunofluorescence experiments of virus infection in the presence of GFP-tagged hVPS4 wt and hVPS4 EQ. For quantitation, >100 cells were scored in each case. (C) Mv 1 Lu cells were transfected with GFP-tagged hVPS4 EQ and then infected with approximately 1–5 pfu/cell influenza virus (WSN). Cells were fixed at 2.5 h post infection and analyzed by confocal microscopy using intrinsic GFP fluorescence (panel a), along with anti-influenza virus NP antibodies (panel b). Panel c represents a merge of the two channels, and a magnified inset is shown to demonstrate colocalization. Bars = 10 μm.

contrast, VSV and SFV appear to require only early endosomes (27). Our data using both MG132 and hVPS4 EQ showed colocalization of influenza vRNPs with defined endosome components, and did not show any obvious arrest at the cell surface. Therefore, we do not consider that ubiquitylation and the vacuolar protein sorting machinery are necessary for virus internalization, but rather for endosomal sorting. The lack of effect of MG132 on SFV and VSV entry would further indicate that the critical sorting event targeted lies beyond the early endosome. Our findings are therefore consistent with an essential role of sorting within the multivesicular body/late endosome during influenza virus entry.

Our data indicate that influenza virus cannot progress along the lysosome-targeted pathway of endocytosis, and is mistargeted in sorting endosomes. We show no significant colocalization with Rab4 or Rab11, which

would normally be considered markers of the recycling pathway. Instead, vRNPs show localization adjacent to Rab9-containing compartments, but no significant colocalization with Rab7 or Rab5. The high degree of colocalization with Rme-1, a protein previously identified as being present in transferrin-positive vesicles (43) as part of the recycling pathway, is somewhat surprising. However in the studies of Lin et al. (43), there was also Rme-1 staining that did not overlap with transferrin in the center of the cell. In the cells used in this study, we did not see any colocalization of Rme-1 with Rab11 or Rab4 (not shown). Our immunofluorescence data showing partial colocalization with M6PR, combined with the GFP-Rab localization would place the MG132-arrested vRNPs within sorting/late endosome domains of the endocytic pathway, rather than in recycling endosomes. Rme-1 has also been shown to have effects on delivery of TGN38 to the TGN, although there is not thought to be any involvement of late endosomes in this case (43). In our cells we have been unable to detect colocalization of vRNPs with TGN markers (not shown).

Although ubiquitin and the vacuolar protein sorting pathway are well known to be involved in endocytosis in the cell, to date viruses (e.g. retroviruses) have only been shown to require these pathways during budding at the cell surface. Ubiquitylation and proteasome activity have been shown to be important for some non-enveloped viruses once they have entered the cytosol (45,46). In this case, ubiquitylation may represent a requirement for proteolysis of capsid component(s) during viral uncoating, and is not thought to involve the vacuolar protein sorting pathway.

Like retroviruses and many other enveloped viruses, influenza virus buds from the plasma membrane, and in principle may require ubiquitin and the vacuolar protein sorting pathway at this point in its life-cycle. However, we show here that this is not the case, confirming the results of others (36). In most cases, the viruses making use of ubiquitin and the vacuolar protein sorting pathway during budding have so-called 'late domains' (e.g. PPPY and PTAP) on their matrix or capsid proteins. Influenza virus does not encode a 'late domain', which may explain the observed differences in the molecular mechanism of virus budding. Interestingly, recombinant influenza viruses have recently been generated which contain a late domain within the viral matrix (M1) protein (47). The late domain substitutions (e.g. PTAP) were designed to replace the basic domain of M1 previously proposed to be involved in nuclear import and/or membrane association (48,49). It will be interesting to examine if these late domain-containing viruses have different requirements for budding from the cell surface.

VPS4 has been shown to be involved in the release of many retroviruses (19,23,24); however, not all retroviruses appear to use the same machinery for budding (35). Another prominent vps component shown to play a role in retrovirus budding is TSG101 (50). However, some retroviruses, notably equine infectious anemia virus (EIAV), show no involvement of TGS101 for budding (22). We also examined the role of TSG101 in influenza virus infection by examining infection in SL6 cells (51), which express mutant TSG101 and have defects in EGF receptor sorting (9). We saw no obvious defect in influenza infection in SL6 cells (not shown) suggesting that VPS4, but not TSG101, is part of the endocytic sorting machinery utilized by influenza virus.

What is the mechanism of action of MG132 during endosomal sorting? In a simple model, MG132 would act by depleting the pool of free ubiquitin in the cytosol and so inhibit monoubiquitylation of a receptor. However, this is considered unlikely, as EGF receptors are efficiently ubiquitylated in the presence of MG132 (8), and under the conditions of MG132 treatment typically used (3 h), there is only a very modest decrease in the pool of ubiquitin in the cell (35). It is possible that there is cross-talk between proteasomal and lysosomal degradation (52). As-yet unidentified proteins that might serve as negative regulators of MVB sorting could be normally inactivated by polyubiquitylation/proteasome function. In this scenario, MG132 would allow maintenance of the activity of a negative regulator of endosomal sorting.

Although we do not formally show a direct role for ubiquitin during influenza entry, it is likely that ubiquitylation is involved during endocytosis of the virus. However, it remains to be determined what component(s) might be the target of the ubiquitylation event. The virus itself is unlikely to be a target for ubiquitylation, as it is present within the endosome itself, and is not exposed to the cytoplasm. If there is a direct monoubiquitylation event occurring, the most likely candidate would be the cytoplasmic tail of the viral receptor. However, the receptor for influenza virus is sialic acid, which can be present on either cell surface glycoprotein or glycolipid (53). In principle, influenza virus might be expected to enter the cell through fluid phase endocytosis. However, a correlation of the data presented here with previous findings with cellular ligands, such as epidermal growth factor, suggests that similar sorting mechanisms are involved. It is possible that an unidentified viral receptor is involved in influenza virus transit through the endosome, which would be the target for ubiquitylation, and that the virus must communicate with specific cellular machinery for intracellular sorting during the initial phase of virus infection.

Materials and Methods

Cells, viruses and infections

Mv 1 Lu cells (American Type Culture Collection, Rockville, MD, USA) were maintained in α-MEM containing 10% calf

serum, 100 U/ml penicillin and 10 μg/ml streptomycin and passaged twice weekly. Influenza A/WSN/33 (H1N1) stocks were grown in MDBK cells, and plaque titered on MDCK cells (54). Semliki Forest virus (SFV) strain M1 was provided by Dr Margaret Kielian, Albert Einstein College of Medicine. VSV (strain *ts*O45) was obtained from the American Type Culture Collection (Rockville, MD, USA). Infections were performed essentially as described previously (55). Briefly, viral stocks were diluted in RPMI 1680 medium containing 0.2% BSA and buffered to pH 6.8 with HEPES, except for VSV which was buffered to pH 6.3. Virus (~1–5 plaque forming units per cell, equivalent to >100 particles per cell) was adsorbed for 90 min at 4 °C, or at 37 °C for 45 min and cells were then maintained in growth medium containing 2% serum at 37 °C. MG132 and lactacystin were obtained from Calbiochem (La Jolla, CA, USA).

Plasmids and transfections

Plasmid DNA encoding GFP-hVPS4 and GFP-hVPS4 EQ, originally cloned in the laboratory of Dr Philip Woodman (University of Manchester, UK) was provided by Dr Becky Craven (Pennsylvania State University). GFP-Rab4 was provided by Dr Marci Scidmore (Cornell University), GFP-Rab7 and GFP-Rab5 were provided by Dr Craig Roy (Yale University), GFP-Rab9 was provided by Dr Suzanne Pfeffer, Stanford University and GFP-Rme-1 was provided by Dr Fred Maxfield (Weill Medical College of Cornell University).

Cells were transfected using an Effectene transfection kit (Qiagen, Valencia CA, USA), or with Lipofectamine 2000 (Invitrogen, Carlsbad CA, USA), according to manufacturers' protocols For transfection, cells were grown on coverslips in 24-well plates and transfected with 0.8–1.0 μg DNA. Transfections were typically allowed to proceed for 16–18 h before analysis, except for Rab expression studies – where cells were analyzed after 5–6 h of transfection to minimize nonspecific localization of the over-expressed Rab protein.

Immunofluorescence microscopy

Preparation of cells for indirect immunofluorescence microscopy was performed as described previously (56). Influenza virus ribonucleoproteins (vRNPs) were detected using the monoclonal antibodies H16, L10–4R5 or 46–4 (American Type Culture Collection, Rockville, MD, USA). VSV was detected with the G protein monoclonal antibody P5D4 (provided by Dr Ira Mellman, Yale University). SFV was detected using an anti E1-1 monoclonal antibody (provided by Dr Margaret Kielian, Albert Einstein College of Medicine). Mannose 6-phosphate receptor (M6PR) was localized using a rabbit polyclonal antibody provided by Dr Bill Brown (Cornell University), early endosome antigen-1 (EEA1) was detected using a monoclonal anti-EEA1 antibody (BD Biosciences Pharmingen, San Diego, CA, USA), and Rab 11 was localized using a monoclonal anti-Rab11 antibody (BD Biosciences Pharmingen). Secondary antibodies used were Alexa 488-labeled (green) or Alexa 568-labeled (red) goat anti-mouse IgG (Molecular Probes, Eugene, OR, USA), using isotype-specific antibodies (anti-mouse IgG1 and IgG2a) where necessary.

For wide-field microscopy, cells were viewed on a Nikon Eclipse E600 fluorescence microscope, using a 40× Plan Apo objective (NA 0.95) or a 20× Plan Apo objective (NA 0.75), and images captured with a SPOT RT camera and SPOT software, version 3.5.4 (Diagnostic Instruments, Sterling Heights, MI, USA) before transfer into Adobe Photoshop (version 7.0). For deconvolution, a 60× Plan Apo objective was used (NA 1.4) for image acquisition and 0.25-μm z-slices collected using QED image software (QED Imaging, Pittsburgh, PA, USA). AutoDeblur Gold (AutoQuant Imaging, Waterlivet, NY, USA) was used for deconvolution, and images transferred into Adobe Photoshop version 7.0 (Adobe Systems, San Jose, CA, USA). For quantitation >100 cells were scored.

Confocal microscopy was performed using an Olympus FluoView confocal station. Alexa 488 was excited with the 488 nm line of an Argon laser and Alexa 568 was excited with the 568 nm line of a Krypton laser. Cells were viewed with a 60× PlanApo objective lens (NA 1.4) and images were captured with FluoView software (Olympus, Melville, NY, USA), before being transferred into Adobe Photoshop (version 7.0).

Flow cytometry

For flow cytometry preparation, cells were detached with 0.2% trypsin/EDTA (Cellgro, Herndon, VA, USA), washed in PBS, fixed in 3% paraformaldehyde/PBS and permeabilized in 0.075% saponin in 10% goat serum/PBS. Cells were incubated with a monoclonal antibody to influenza virus neuraminidase (NA) (H17, L17 5R17, kindly provided by Dr Jonathan Yewdell, NIH) for 30 min, followed by Alexa 488-labeled goat anti-mouse IgG for 30 min. Cells were analyzed on a FACSCalibur cytometer and data collected using CellQuest 3.1f software (Becton Dickinson Immunocytometry Systems, San Jose, CA, USA). Data analysis was performed using FlowJo 4.3 software (Tree Star Inc., San Carlos, CA, USA) At least 10 000 cells were analyzed for each sample.

Hemagglutination assay

Freshly isolated chicken blood was washed 3× with PBS and red blood cells were resuspended in PBS at a concentration of 1%. Influenza virus dilutions (50 μl) were made in PBS, and 50 μl of red blood cell suspension was added to individual wells in a 96-well plate and allowed to settle for 45 min. Wells were judged to be HA-negative (no agglutination of red cells) if a dot/pellet of red cells was present, and positive (red cells agglutinated by HA) if a smooth suspension of red cells was present.

Acknowledgments

We thank Ruth Collins for helpful discussions throughout the course of this work and Beverley Bauman and Damon Ferguson for excellent technical assistance. We also thank Jon Yewdell, Ira Mellman, Margaret Kielian, Bill Brown, Craig Roy, Marci Scidmore, Suzanne Pfeffer, Philip Woodman, Becky Craven and Fred Maxfield for their kind contributions of reagents, and Volker Vogt and Colin Parrish for helpful advice. This work was supported by a Scientist Development Grant from the American Heart Association and by grant R01AI48678 from the National Institutes of Health (to G.R.W.).

References

1. Voges D, Zwickl P, Baumeister W. The 26S proteasome: a molecular machine designed for controlled proteolysis. Annu Rev Biochem 1999;68:1015–1068.
2. Hicke L. Protein regulation by monoubiquitin. Nat Rev Mol Cell Biol 2001;2:195–201.
3. Terrell J, Shih S, Dunn R, Hicke L. A function for monoubiquitination in the internalization of a G protein-coupled receptor. Mol Cell 1998;1:193–202.
4. Katzmann DJ, Odorizzi G, Emr SD. Receptor downregulation and multivesicular-body sorting. Nat Rev Mol Cell Biol 2002;3:893–905.
5. Wendland B, Emr SD, Riezman H. Protein traffic in the yeast endocytic and vacuolar protein sorting pathways. Curr Opin Cell Biol 1998;10:513–522.
6. Stahl PD, Barbieri MA. Multivesicular bodies and multivesicular endosomes: the 'ins and outs' of endosomal traffic. Sci STKE 2002; 2002: PE32.
7. Strous GJ, Govers R. The ubiquitin-proteasome system and endocytosis. J Cell Sci 1999;112:1417–1423.
8. Longva KE, Blystad FD, Stang E, Larsen AM, Johannessen LE, Madshus IH. Ubiquitination and proteasomal activity is required for transport of the EGF receptor to inner membranes of multivesicular bodies. J Cell Biol 2002;156:843–854.
9. Babst M, Odorizzi G, Estepa EJ, Emr SD. Mammalian tumor susceptibility gene 101 (TSG101) and the yeast homologue, Vps23p, both function in late endosomal trafficking. Traffic 2000;1:248–258.
10. Rocca A, Lamaze C, Subtil A, Dautry-Varsat A. Involvement of the ubiquitin/proteasome system in sorting of the interleukin 2 receptor beta chain to late endocytic compartments. Mol Biol Cell 2001;12:1293–1301.
11. Sachse M, Urbe S, Oorschot V, Strous GJ, Klumperman J. Bilayered clathrin coats on endosomal vacuoles are involved in protein sorting toward lysosomes. Mol Biol Cell 2002;13:1313–1328.
12. Sachse M, van Kerkhof P, Strous GJ, Klumperman J. The ubiquitin-dependent endocytosis motif is required for efficient incorporation of growth hormone receptor in clathrin-coated pits, but not clathrin-coated lattices. J Cell Sci 2001;114:3943–3952.
13. Shenoy SK, McDonald PH, Kohout TA, Lefkowitz RJ. Regulation of receptor fate by ubiquitination of activated beta 2-adrenergic receptor and beta-arrestin. Science 2001;294:1307–1313.
14. Perez OD, Nolan GP. Resistance is futile: assimilation of cellular machinery by HIV-1. Immunity 2001;15:687–690.
15. Jayakar HR, Murti KG, Whitt MA. Mutations in the PPPY motif of vesicular stomatitis virus matrix protein reduce virus budding by inhibiting a late step in virion release. J Virol 2000;74:9818–9827.
16. Craven RC, Harty RN, Paragas J, Palese P, Wills JW. Late domain function identified in the vesicular stomatitis virus M protein by use of rhabdovirus-retrovirus chimeras. J Virol 1999;73:3359–3365.
17. Vogt VM. Ubiquitin in retrovirus assembly: actor or bystander? Proc Natl Acad Sci USA 2000;97:12945–12947.
18. Timmins J, Schoehn G, Ricard-Blum S, Scianimanico S, Vernet T, Ruigrok RW, Weissenhorn W. Ebola virus matrix protein VP40 interaction with human cellular factors Tsg101 and Nedd4. J Mol Biol 2003;326:493–502.
19. Licata JM, Simpson-Holley M, Wright NT, Han Z, Paragas J, Harty RN. Overlapping motifs (PTAP and PPEY) within the Ebola virus VP40 protein function independently as late budding domains: involvement of host proteins TSG101 and VPS-4. J Virol 2003;77:1812–1819.
20. Maeda A, Lee BH, Yoshimatsu K, Saijo M, Kurane I, Arikawa J, Morikawa S. The intracellular association of the nucleocapsid protein (NP) of Hantaan virus (HTNV) with small ubiquitin-like modifier-1 (SUMO-1) conjugating enzyme 9 (Ubc9). Virology 2003;305:288–297.
21. Harty RN, Brown ME, McGettigan JP, Wang G, Jayakar HR, Huibregtse JM, Whitt MA, Schnell MJ. Rhabdoviruses and the cellular ubiquitin-proteasome system: a budding interaction. J Virol 2001;75: 10623–10629.
22. Tanzi GO, Piefer AJ, Bates P. Equine infectious anemia virus utilizes host vesicular protein sorting machinery during particle release. J Virol 2003;77:8440–8447.
23. Martin-Serrano J, Zang T, Bieniasz PD. Role of ESCRT-I in retroviral budding. J Virol 2003;77:4794–4804.
24. Garrus JE, von Schwedler UK, Pornillos OW, Morham SG, Zavitz KH, Wang HE, Wettstein DA, Stray KM, Cote M, Rich RL, Myszka DG, Sundquist WI. Tsg101 and the vacuolar protein sorting pathway are essential for HIV-1 budding. Cell 2001;107:55–65.
25. Sieczkarski SB, Whittaker GR. Dissecting virus entry via endocytosis. J Gen Virol 2002;83:1535–1545.
26. Russell DG, Marsh M. Endocytosis in pathogen entry and replication. In: Marsh M, ed. Endocytosis. Oxford: Oxford University Press; 2001. pp 247–280.
27. Sieczkarski SB, Whittaker GR. Differential requirements of Rab5 and Rab7 for endocytosis of influenza and other enveloped viruses. Traffic 2003;4:333–343.
28. Helenius A. Semliki Forest virus penetration from endosomes: a morphological study. Biol Cell 1984;51:181–185.
29. Lee DH, Goldberg AL. Proteasome inhibitors: valuable new tools for cell biologists. Trends Cell Biol 1998;8:397–403.
30. van Kerkhof P, Alves dos Santos CM, Sachse M, Klumperman J, Bu G, Strous GJ. Proteasome inhibitors block a late step in lysosomal transport of selected membrane but not soluble proteins. Mol Biol Cell 2001;12:2556–2566.
31. Schubert U, Ott DE, Chertova EN, Welker R, Tessmer U, Princiotta MF, Bennink JR, Krausslich HG, Yewdell JW. Proteasome inhibition interferes with gag polyprotein processing, release, and maturation of HIV-1 and HIV-2. Proc Natl Acad Sci USA 2000;97:13057–13062.
32. Strack B, Calistri A, Accola MA, Palu G, Gottlinger HG. A role for ubiquitin ligase recruitment in retrovirus release. Proc Natl Acad Sci USA 2000;97:13063–13068.
33. Patnaik A, Chau V, Wills JW. Ubiquitin is part of the retrovirus budding machinery. Proc Natl Acad Sci USA 2000;97:13069–13074.
34. Bishop N, Horman A, Woodman P. Mammalian class E vps proteins recognize ubiquitin and act in the removal of endosomal protein-ubiquitin conjugates. J Cell Biol 2002;157:91–101.
35. Ott DE, Coren LV, Sowder RC, 2nd, Adams J, Schubert U. Retroviruses have differing requirements for proteasome function in the budding process. J Virol 2003;77:3384–3393.
36. Hui EK, Nayak DP. Role of ATP in influenza virus budding. Virology 2001;290:329–341.
37. Marsh M, Helenius A. Virus entry into animal cells. Adv Virus Res 1989;36:107–151.
38. Collins RN, Brennwald P. Rab. In: Hall A, ed. Gtpases. Oxford: Oxford University Press; 2000. pp 137–175.
39. Pfeffer SR. Rab GTPases: specifying and deciphering organelle identity and function. Trends Cell Biol 2001;11:487–491.
40. Somsel Rodman J, Wandinger-Ness A. Rab GTPases coordinate endocytosis. J Cell Sci 2000;113:183–192.

41. Lombardi D, Soldati T, Riederer MA, Goda Y, Zerial M, Pfeffer SR. Rab9 functions in transport between late endosomes and the trans Golgi network. EMBO J 1993;12:677–682.
42. Barbero P, Bittova L, Pfeffer SR. Visualization of Rab9-mediated vesicle transport from endosomes to the trans-Golgi in living cells. J Cell Biol 2002;156:511–518.
43. Lin SX, Grant B, Hirsh D, Maxfield FR. Rme-1 regulates the distribution and function of the endocytic recycling compartment in mammalian cells. Nat Cell Biol 2001;3:567–572.
44. Bishop N, Woodman P. ATPase-defective mammalian VPS4 localizes to aberrant endosomes and impairs cholesterol trafficking. Mol Biol Cell 2000;11:227–239.
45. Galinier R, Gout E, Lortat-Jacob H, Wood J, Chroboczek J. Adenovirus protein involved in virus internalization recruits ubiquitin-protein ligases. Biochemistry 2002;41:14299–14305.
46. Ros C, Burckhardt CJ, Kempf C. Cytoplasmic trafficking of minute virus of mice: low-pH requirement, routing to late endosomes, and proteasome interaction. J Virol 2002;76:12634–12645.
47. Hui EK, Barman S, Yang TY, Nayak DP. Basic residues of the helix six domain of influenza virus M1 involved in nuclear translocation of M1 can be replaced by PTAP and YPDL late assembly domain motifs. J Virol 2003;77:7078–7092.
48. Ruigrok RWH, Barge A, Durrer A, Brunner J, Ma K, Whittaker GR. Membrane interaction of influenza M1 protein. Virology 2000;267: 1781–1786.
49. YeZ, Robinson D, Wagner RR. Nucleus-targeting domain of the matrix protein (M1) of influenza virus. J Virol 1995;69:1964–1970.
50. Freed EO. The HIV–TSG101 interface: recent advances in a budding field. Trends Microbiol 2003;11:56–59.
51. Li L, Cohen SN. Tsg101. a novel tumor susceptibility gene isolated by controlled homozygous functional knockout of allelic loci in mammalian cells. Cell 1996;85:319–329.
52. Raiborg C, Rusten TK, Stenmark H. Protein sorting into multivesicular endosomes. Curr Opin Cell Biol 2003;15:1–10.
53. Skehel JJ, Wiley DC. Receptor binding and membrane fusion in virus entry: the influenza hemagglutinin. Annu Rev Biochem 2000;69: 531–569.
54. Mahy BWJ. Virology: A Practical Approach. Oxford: IRL Press; 1985.
55. Root CR, Wills EG, McNair LL, Whittaker GR. Entry of influenza viruses into cells is inhibited by a highly specific protein kinase C inhibitor. J Gen Virol 2000;81:2697–2705.
56. Whittaker G, Kemler I, Helenius A. Hyperphosphorylation of mutant influenza virus matrix (M1) protein causes its retention in the nucleus. J Virol 1995;69:439–445.